machines

MDPI

Article

Highly Stable Switchable Emissions of an Erbium-Doped Fiber Ring Laser Using Cascaded MZIs Based on CHCF

Luis A. Herrera-Piad [1], Sigifredo Marrujo-García [2], Iván Hernández-Romano [3,*], Daniel A. May-Arrioja [4], Vladimir P. Minkovich [5] and Miguel Torres-Cisneros [2]

1 Mechatronics Department, Universidad Tecnológica de Aguascalientes, Blvrd Juan Pablo II, Aguascalientes 20200, Mexico
2 Electronics Department, DICIS, Universidad de Guanajuato, Carretera Salamanca-Valle de Santiago km 3.5 + 1.8, Salamanca 36885, Mexico
3 CONACYT-Electronics Department, DICIS, Universidad de Guanajuato, Carretera Salamanca-Valle de Santiago km 3.5 + 1.8, Salamanca 36885, Mexico
4 Fiber and Integrated Optics Laboratory (FIOLab), Centro de Investigaciones en Optica A.C., Aguascalientes 20200, Mexico
5 Centro de Investigaciones en Optica A.C., Calle Lomas del Bosque 115, Leon 37150, Mexico
* Correspondence: hromano@ugto.mx

Abstract: A stable, single, and dual-wavelength erbium-doped fiber laser (EDFL), based on two Mach–Zehnder interferometers (MZIs), arranged in a cascade configuration, was proposed for experimental purposes. Both MZIs were assembled by splicing a capillary hollow-core fiber (CHCF) section between two multimode fibers (MMFs) segments. The novelty of this single and dual-wavelength EDFL is that the switchable operation of the laser is achieved by thermally tuning the interference pattern of one MZI and not by adjusting the polarization state inside the fiber ring cavity. The maximum measured value of SNR was 58.9 dB for the single and dual-wavelength laser emissions. Moreover, the stable output power exhibited by this EDFL, in terms of minimal power and wavelength fluctuations, at 0.05 dB and 10 pm, was detected during the single and dual-wavelength operation. It is worth noticing that switching is achieved at exact wavelength locations with a separation of 1.8 nm and not randomly, as reported by other works. These features make this switchable EDFL an appealing candidate for application in optical fiber communication systems and fiber sensing.

Keywords: erbium-doped fiber laser; Mach-Zehnder interferometer; multiwavelength laser emission; capillary hollow core fiber (CHCF)

check for updates

Citation: Herrera-Piad, L.A.; Marrujo-García, S.; Hernández-Romano, I.; May-Arrioja, D.A.; Minkovich, V.P.; Torres-Cisneros, M. Highly Stable Switchable Emissions of an Erbium-Doped Fiber Ring Laser Using Cascaded MZIs Based on CHCF. *Machines* **2022**, *10*, 962. https://doi.org/10.3390/machines10100962

Academic Editor: Dan Zhang

Received: 26 September 2022
Accepted: 17 October 2022
Published: 21 October 2022

Publisher's Note: MDPI stays neutral with regard to jurisdictional claims in published maps and institutional affiliations.

1. Introduction

In the last two decades, multiwavelength erbium-doped fiber lasers (EDFLs) have become reliable light sources for different applications such as wavelength division multiplexing [1,2], optical fiber sensing [3,4], and microwave photonics [5,6], to mention but a few. As is well known, homogeneous line broadening produces high mode competition, thus causing the generation of unstable emissions in multiwavelength EDFLs [7–9]. One possible solution to this problem is to use fiber wavelength filters; most of them work similarly to Sagnac [10], Fabry–Perot [11], and Mach–Zehnder [12] interferometers, though other filters based on different fiber structures can also be used [13–22]. Among these devices, the Mach–Zehnder interferometers (MZIs) have attracted significant attention due to their simple structure and the ease with which they can be manufactured; therefore, different optical fibers and fiber structures have been used to implement these interferometers. For instance, Y. Lv et al. [23] proposed a Mach–Zehnder interferometer (MZI) that was based on a triple-core photonic crystal fiber in order to implement a single, dual, and triple-wavelength EDFL. In this case, the total length of the fiber structure, including the length of the multimode fiber (MMF) that acts as a modal coupler, was 5.9 cm. They

reported a side-mode suppression ratio (SMSR) of 50, 45, and 37 dB for single, dual, and triple-wavelength emissions, respectively, and the measured 3 dB linewidth was 0.026 nm for all cases. The maximum power fluctuation for single, dual, and triple-wavelength emissions were 0.44, 0.77, and 0.96 dB, respectively. Moreover, Y. Qi et al. [24] proposed a single, dual, and triple-wavelength EDFL, wherein the switchable operation of this laser depended on an MZI that was constructed using the core-offset technique where 57 cm of few-mode fiber was spliced between two single-mode fibers (SMF). They reported a maximum signal–noise ratio (SNR) of 54, 43, and 49 dB for single, dual, and triple-wavelength emission, respectively, and the measured 3 dB linewidth was 0.02 nm for all cases. The maximum power fluctuation for the single, dual, and triple-wavelength emissions were 1.14, 2, and 4.33 dB, respectively. Additionally, J. A. Martin-Vela et al. [12] proposed an MZI based on the core-offset technique where the sensing SMF, with 5 cm of length, was covered with Al that was 30 nm thick, in order to construct a single, dual, and triple-wavelength EDFL. They reported a maximum SMSR of 55, 50, and 50 dB for single, dual, and triple-wavelength emissions, respectively, and the measured 3 dB linewidth of the single-wavelength emission was 0.02 nm (the other linewidths were not reported). The maximum peak power fluctuation for the single, dual, and triple-wavelength emissions were 0.2, 1, and 5 dB, respectively. In the three examples mentioned above, the multiwavelength lasing operation was achieved by adjusting the polarization controller (PC) that was inside the laser cavity. Changing the polarization alters the gain and loss inside the cavity, and it modifies the interference pattern of each MZI that was used in these examples. It is worth mentioning that the number of wavelengths that are capable of lasing is determined by the peaks of maximum transmission in the fringe pattern of the MZI. For example, if a single-wavelength emission switches to a dual-wavelength emission by adjusting the PC, this dual operation could be due to the occurrence of two consecutive peaks in the fringe pattern (i.e., the wavelength spacing between these laser emissions are equal to the free spectrum range (*FSR*) of the interference pattern); however, if the laser switched to single-wavelength emissions, and then came back to using a dual operation, it is possible that the lasing peaks would not be consecutive. This problem can be solved by adjusting the polarization state to obtain the same result, but it requires more time. In our view, adjusting the polarization state until a specific lasing peak appears is time-consuming and it exhibits low control of the multiwavelength laser emissions in real-time.

On the other hand, several authors have proposed using two wavelength filters in a cascade configuration inside an EDFL, in a ring configuration, in order to obtain multiwavelength laser emissions with narrower linewidths, better stability, and higher SMSR [25–30]. For example, Z. Tang et al. [25] manufactured two MZIs that were set in an EDFL to implement a single and dual-wavelength laser. The first MZI was constructed by splicing a 11.2 cm segment of two core photonic crystal fibers between two SMF segments, and its *FSR* was approximately 25 nm. The second interferometer was constructed using two conventional fiber couplers to assemble an MZI, and the path difference of the two arms was 2.1 mm, with an *FSR* of 0.78 nm. We should mention that the last interferometer is usually large, and the arms' lengths are approximately two meters. They reported an SMSR of 45 and 42 dB for single and dual-wavelength emissions, respectively, and the measured 3 dB linewidths of the single and dual-wavelength emissions were 0.026 and 0.03 nm, respectively. The maximum power fluctuation for single and dual-wavelength emissions was 0.47, 2, and 0.8 dB, respectively. Additionally, L. Zhang et al. [28] proposed using two MZIs to implement a single and dual-wavelength EDFL. The first MZI was manufactured by tapering a seven-core fiber (waist of 8.2 µm, waist length of 8 mm) with an *FSR* of 13.93 nm. As in the previous example, the second MZI was constructed using two conventional fiber couplers to generate an *FSR* of 0.37 nm. For single and dual-wavelength emissions, they reported that the values of the SMSR, linewidth, and maximum peak power fluctuation were 45 dB, 0.0171 nm, and 0.155 dB, respectively. It is worth noting that by adjusting the PC inside the cavity, multiwavelength emissions were obtained, as was also the case in the configuration where they used one interferometer. Another drawback shown

in these examples is the assembly of MZI using conventional couplers, as it makes the laser more complex and bulkier.

In this paper, a stable single and dual-wavelength EDFL, based on two cascaded MZIs, was proposed and experimentally investigated. The all-fiber MZIs were constructed by splicing a section of a capillary hollow core fiber (CHCF) between two segments of MMF. The maximum length of these MZIs was 5 mm, making these interferometers attractive due to their easy construction, small size, low cost, and sturdiness. Moreover, the MZI with the longer *FSR* was used as the wavelength selector, whereas the MZI with the smaller *FSR* exhibits narrower linewidth emissions and determines the separation of switchable steps. The novelty of this single and dual-wavelength EDFL is that the switchable operation of the laser is achieved by thermally tuning the interference pattern of one MZI and not by adjusting the polarization state inside the fiber ring cavity, as in the examples mentioned above. This scheme provides a simple way to switch wavelengths over well-known wavelength locations (peak emissions), thus eliminating the randomness obtained via polarization tuning. The maximum measured value of SNR was 58.9 dB for the single and dual-wavelength laser emissions, and the linewidth for all the peaks was 30 pm. Moreover, no power and wavelength fluctuations were detected during the single and dual-wavelength operation, thus making the laser emissions of this switchable EDFL highly stable.

2. Materials and Methods

A fiber ring laser cavity was assembled, as shown in Figure 1, using a pump laser diode (BL976-PAG700, Thorlabs, Newton, NJ, USA) that coupled light to a 980/1550 wavelength division multiplexer (WDM) fiber coupler. A 2 m long segment of EDF (Er80-8/125, Thorlabs, Newton, NJ, USA) was used as the gain medium, and it was pumped with the light of the laser diode at a wavelength of 976 nm. A PC and an isolator were added to the laser cavity to obtain a better SNR and to observe the unidirectional operation, respectively. To monitor the laser output, an optical fiber coupler (90/10) was set into the cavity; the 10% port was connected to the OSA, and the 90% port was used to close the cavity for continuous laser generation. Moreover, to develop a switchable EDFL, two MZIs that worked similarly to filters were placed into the laser cavity. Their fabrication process and working principle are described in the next section.

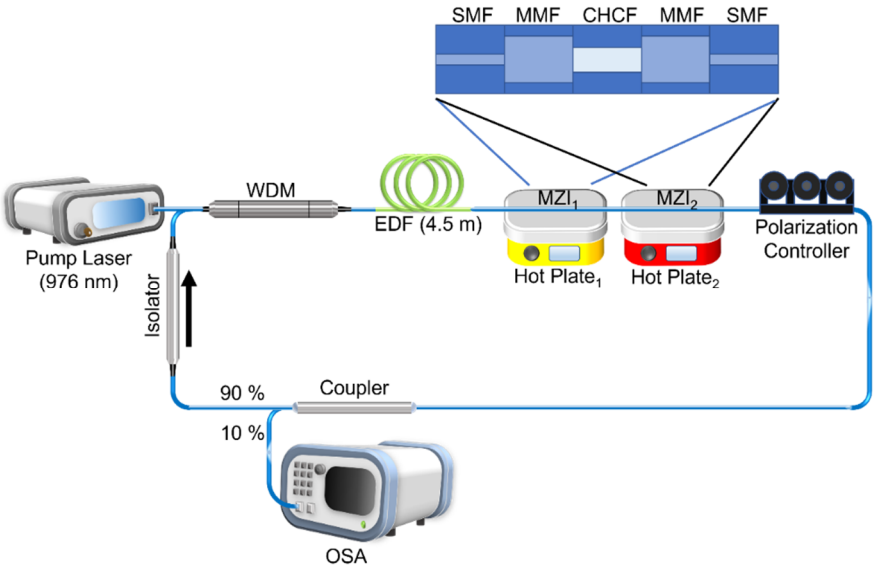

Figure 1. Schematic of the fiber ring laser using two cascaded MZIs.

Fabrication Process and Working Principle

The structure of these filters consisted of a spliced segment of CHCF (whose inner and outer diameters are 62.5 and 125 µm, respectively) between two pieces of 1 mm of MMF (105/125 µm), and this fiber structure was sandwiched between two conventional SMF (see Figure 1). The CHCF was composed of SiO_2, and its coating was composed of UV-cured acrylate (not commercial fiber). It should be noted that the coatings of the CHCF and MMF were removed before starting the construction process, and the SMF was handled as a standard splice. It is crucial to note that MMF segments work similarly to mode couplers, sending light toward the hollow core and the ring cladding of the CHCF. The equation that describes the output signal of this MZI is [31]

$$I = I_1 + I_2 + \sqrt{I_1 I_2} cos\left(2\pi \Delta n_{eff} L/\lambda\right), \quad (1)$$

where I_1 and I_2 are the intensities of the light in the hollow core and the ring cladding, respectively. L, λ, and Δn_{eff} are the length of the MZI, the wavelength of the light, and the effective refractive index difference between the modes that travel in the CHCF (a detailed explanation can be found in [31]), respectively. Moreover, the *FSR* of the output signal of this MZI can be calculated using $FSR = \lambda^2/\Delta n_{eff} L$, and one may observe that it is feasible to change the *FSR* of the interference pattern by modifying the length of the CHCF. We constructed four MZIs with different *FSR* values by taking advantage of this property and our capability of cutting CHCF segments with high precision. Implementing a switchable laser requires two MZIs set into a fiber laser cavity in a cascade configuration. One of these devices (MZI_1) had an *FSR* that was higher than 10 nm, and the other (MZI_2) had an *FSR* that was lower than 2 nm. For the MZI_1, three MZIs were constructed, and their *FSRs* are 17.82, 13.29, and 10.98 nm (see Figure 2d), which correspond to the estimated lengths of 0.3, 0.4, and 0.5 mm, respectively. The MZIs with lengths of 0.3, 0.4, and 0.5 will be named MZI_{1a}, MZI_{1b}, and MZI_{1c}, respectively. For the MZI_2, one MZI was constructed, and its *FSR* was 1.8 nm (see Figure 2d), corresponding to an estimated length of 3 mm. A picture of the MZIs that were used in this experiment is shown in Figure 3. Table 1 shows the essential features of the MZIs.

Table 1. Characteristics of the MZIs.

	Experimental *FSR* (nm)	**Calculated Length * (mm)**	**Designed CHCF Length (mm)**	**Error (%)**	**Contrast (dB)**
MZI_{1a}	17.8	0.304	0.3	1.33	42.2
MZI_{1b}	13.3	0.407	0.4	1.75	19.7
MZI_{1c}	11.0	0.493	0.5	1.40	19.0
MZI_2	1.8	2.942	3	1.93	15.4

* This value was calculated using the experimental *FSR* and the equation ($FSR = \lambda^2/\Delta n_{eff} L$).

It should be noted that we previously reported [32] on a tunable erbium-doped fiber ring laser using an MZI based on CHCF. In that work, we demonstrate that the spectral response of the MZI undergoes a redshift as the temperature increases, with a slope of 33 pm/°C. This thermal tunability allowed us to use two MZIs in a fiber ring laser cavity, using the MZI_1 as a wavelength selector (larger *FSR*); conversely, MZI_2 was used as a reference device in a steady state condition. In other words, the interference pattern of the MZI_1 tunes over the spectrum of the MZI_2 to choose a peak (at a specific wavelength), or peaks (multi-wavelengths), that will emit laser light. It should be noted that the MZI_2 determines the switchable step (*FSR* = 1.8 nm), as well as the narrower laser linewidth when the two MZIs are connected in a cascade configuration. Moreover, all the MZIs that were used in this experiment are polarization-independent elements; this means that the amplitude and phase of their output fringing patterns do not change with the input polarization state of light.

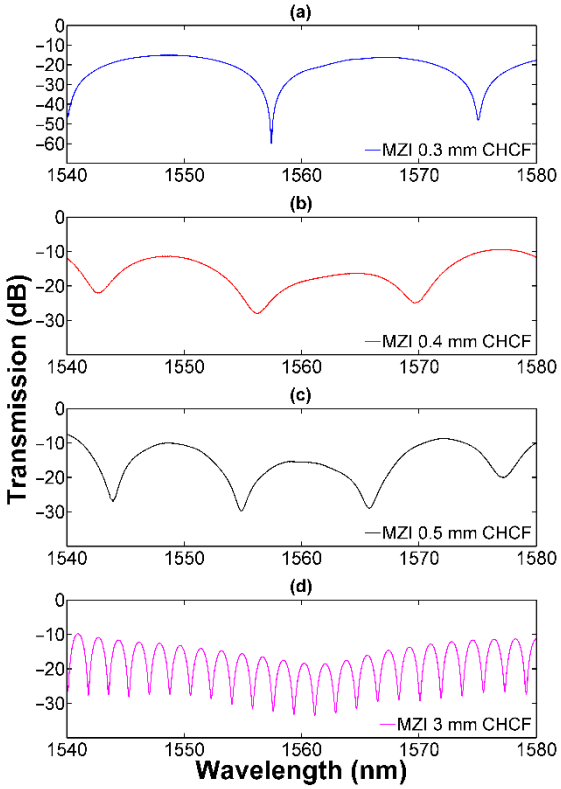

Figure 2. Measured transmission spectra and corresponding *FSR* of (**a**) MZI_{1a} (17.82 nm), (**b**) MZI_{1b} (13.29 nm), (**c**) MZI_{1c} (10.98 nm), and (**d**) MZI_2 (1.8 nm).

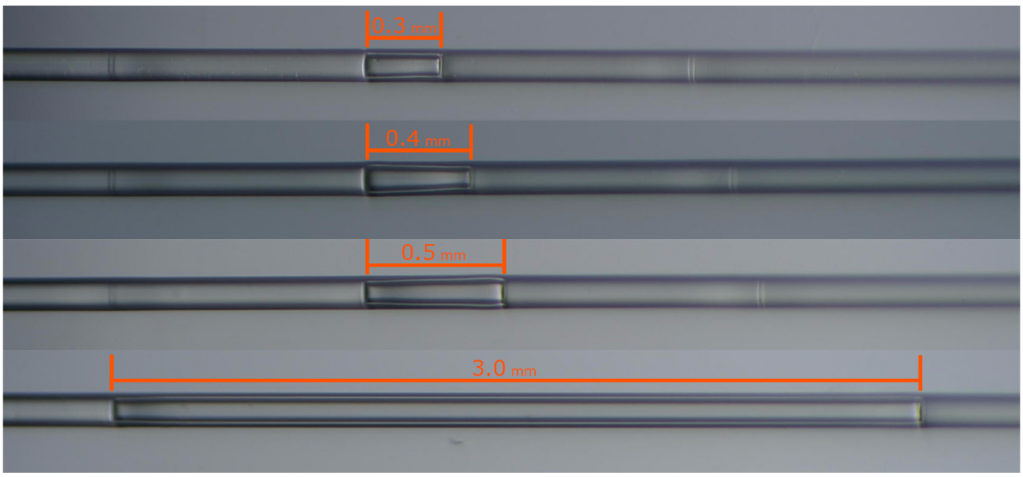

Figure 3. A microscope image of the four MZIs used in this experiment.

The spectral responses of the cascade combination of MZI_{1a}, MZI_{1b}, and MZI_{1c}, with the MZI_2, are shown in Figure 4. These transmission spectra were taken using the amplified spontaneous emission (ASE) of the Erbium-doped fiber (in an open cavity) when the pump power was fixed at 250 mW. In these three cases, the interference pattern of the MZI_2 was modulated by the signal generated by MZI_{1a}, MZI_{1c}, and MZI_{1c}, respectively (see black curves in Figure 3). For a better understanding, the peaks that show the maximum transmission in the interference pattern were produced by two cascaded MZIs, which were marked to indicate that they were highly likely to produce a laser emission. The wavelengths of the peaks were measured, and the results are shown in Table 2.

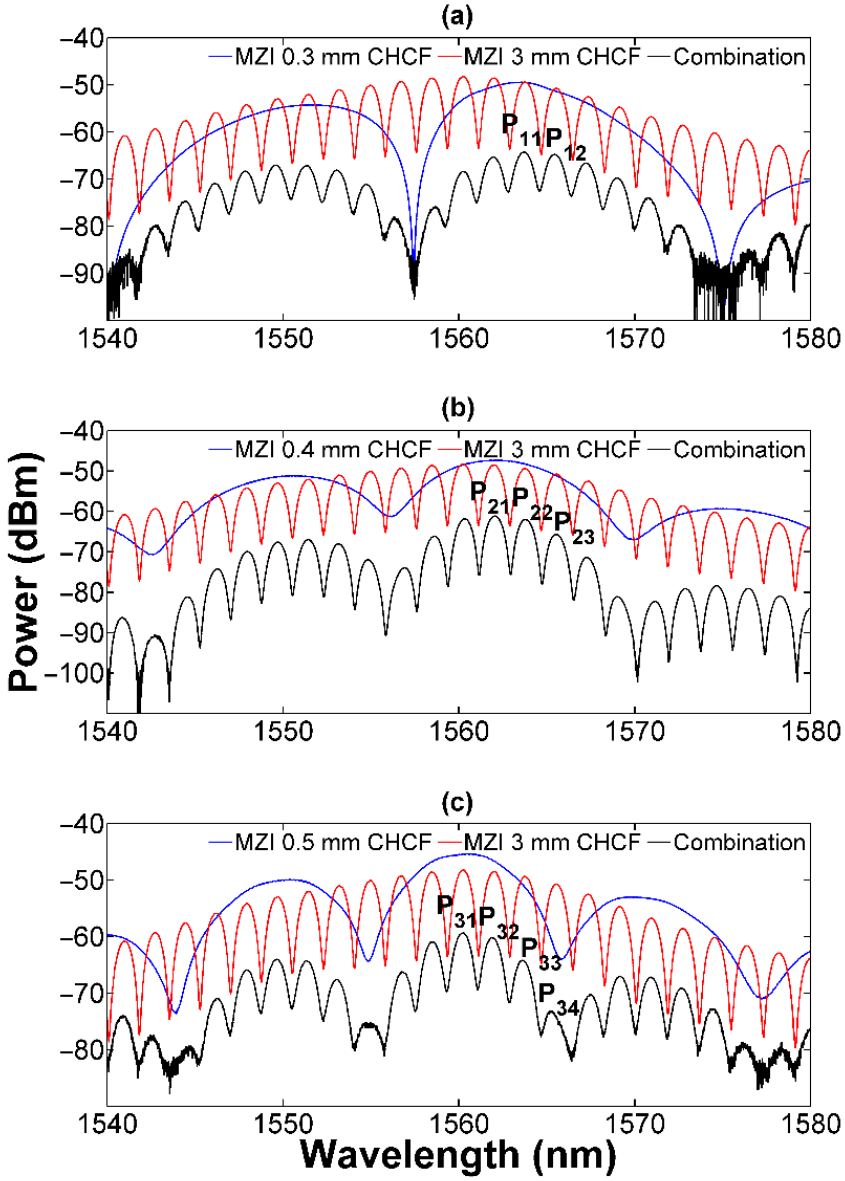

Figure 4. Measured transmission spectra of the MZI_2 connected in a series (Cascade configuration) with the (**a**) MZI_{1a}, (**b**) MZI_{1b}, and (**c**) MZI_{1c}.

Table 2. Measured transmission spectra of the MZI_2 connected in series with the (a) MZI_{1a}, (b) MZI_{1b}, (c) MZI_{1c}, and (d) MZI_2 (cascade configuration).

Cascaded MZIs	Peak	Wavelength (nm)
MZI_2 and MZI_{1a}	P_{11}	1563.7
	P_{12}	1565.5
MZI_2 and MZI_{1b}	P_{21}	1562.7
	P_{22}	1564.5
	P_{23}	1566.3
MZI_2 and MZI_{1c}	P_{31}	1560.0
	P_{32}	1561.8
	P_{33}	1563.6
	P_{34}	1565.4

3. Results

An experimental study was carried out to analyze the switchable operation of an EDFL using two MZIs connected in a series configuration, see Figure 1. Three cases were investigated; this includes the combination of the MZI_2 with the MZI_{1a}, MZI_{1b}, and MZI_{1c}, respectively. It should be mentioned that changing the order of the MZI_2 and MZI_1 (in the three cases) does not affect the performance of the laser, as we observed in the experiments. The MZI_2 was set on a hot plate (Echotherm, Model IC20) at a constant temperature, 20 °C, whereas the MZI_1 was on a hot plate (Thermo Scientific™, model HP88854100, Waltham, MA, USA) that underwent different temperatures; this produced the interference pattern of the MZI_1 which suffered a redshift. In the following sections, the results of the three cases are shown.

3.1. MZI_2 and MZI_{1a} in a Cascade Configuration

The transmission spectrum of the cascaded MZI_2 and MZI_{1a} is shown in Figure 4a. This indicated that the laser emission of this EDFL would probably occur at P_{11}, since this peak shows the highest transmission. When these two cascade interferometers were set in the laser cavity (see Figure 1) both interferometers were at 20 °C, the polarization controller was properly adjusted, and the pump power was fixed at 250 mW to obtain the maximum SNR at room temperature. All measurements were acquired using this pump power. In this scenario, we observed a laser emission of 1563.7 nm (P_{11}), with an SNR of 58.9 dB, as shown in Figure 5a. The temperature of the MZI_{1a} was then increased in increments of 1 °C, from 20 °C to 29 °C, and it was observed that the single-wavelength laser emission remained fixed at 1563.7 nm (P_{11}) within this temperature range. Nevertheless, when the MZI_{1a} temperature reached 30 °C, another laser emission appeared at 1565.5 nm (P_{12}) with an SNR of 58.6 dB. This dual-wavelength laser emission was achieved because the peak of the MZI_{1a}, with a large *FSR*, was tuned to the point where peaks P_{11} and P_{12}, from the MZI_2, which had small *FSRs*, exhibited the same intensity after a round trip. In such scenarios, those peaks are enhanced, and they eventually achieve laser emissions. Since this condition was achieved due to the shape of the tuning peak from MZI_{1a}, the dual-wavelength emission was observed within a narrower temperature range, as shown in Figure 5. This dual-wavelength laser emission continued until the MZI_{1a} reached a temperature of 40 °C, and at that point, at P_{12}, the EDFL switched to single-wavelength laser emissions. The laser emission at P_{12} remained fixed when the temperature of the MZI_{1a} varied between 40 to 160 °C, as can be seen in Figure 5a. The linewidth of the P_{11} and P_{12} was 0.03 nm. Furthermore, the wavelength stability of these laser emissions against temperature changes was measured and it is presented in Figure 5b. In the case of single-wavelength laser emissions, the peaks P_{11} and P_{12} did not vary their amplitudes and positions as the temperature changed from 20 to 29 °C and from 40 to 160 °C, respectively. In the case of dual-wavelength laser emissions, the peaks P_{11} and P_{12} did not modify their amplitudes and positions as the temperature changed from 30 to 39 °C. This means that the MZI_{1a} can undergo temperature fluctuations of up 9 °C, and the laser emission (single/dual) will not suffer changes in terms of their amplitudes or positions (wavelengths). This also indicates that for real applications, the temperature controller used to set the temperature on the MZI_{1a} does not require high accuracy. Similar behaviors are observed in the other two cases (MZI_{1b} and MZI_{1c}) (see the following sections for more information).

3.2. MZI_2 and MZI_{1b} in a Cascade Configuration

Since the peak (P_{21}) shows the highest transmission, as is shown in Figure 4b, the laser emission is likely to occur at that peak. In the laser cavity, these two interferometers were 20 °C and connected in a series configuration (see Figure 1). Laser emission was detected at 1562.7 nm (P_{21}), with an SNR of 50.3 dB, as shown in Figure 6a, when the pump power was fixed at 250 mW. As with the previous case, a similar analysis was carried out by increasing the temperature of the MZI_{1b} in increments of 1 °C, from 20 to 160 °C (see Figure 6a,b).

The linewidth of the P_{21}, P_{12}, and P_{23} was 0.03 nm. The overall measurement results are summarized in Table 3.

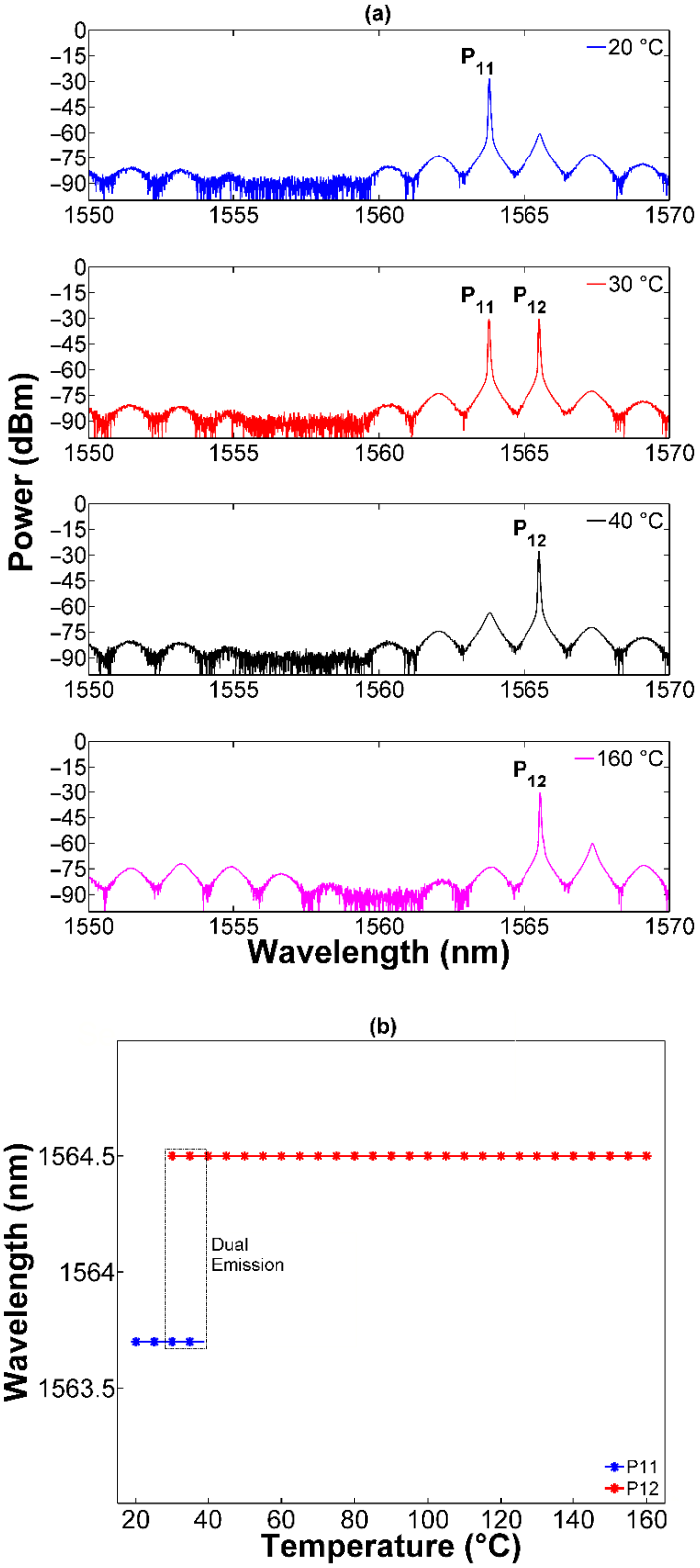

Figure 5. Switchable operation of the EDFL using MZI_2 and MZI_{1a} in a cascade configuration, withstanding temperature variations between 20 to 160 °C. (**a**) Laser emissions and (**b**) stability analysis of laser emissions against temperature changes.

Table 3. Summarized results of the MZI_2 connected and cascaded with MZI_1.

Cascaded MZIs	Temperature (°C)	Single-Wavelength Laser Emission (nm)	Dual-Wavelength Laser Emission	SNR (dB)
MZI_2 and MZI_{1a}	20–29	P_{11} (1563.7)		58.9
	30–39		P_{11} and P_{12}	58.9 and 58.6
	40–160	P_{12} (1565.5)		58.6
MZI_2 and MZI_{1b}	20–79	P_{21} (1562.7)		50.3
	80–89		P_{21} and P_{22}	50.3 and 50.9
	90–149	P_{22} (1564.5)		50.9
	150–159		P_{22} and P_{23}	50.9 and 50.8
	160	P_{23} (1566.3)		50.8
MZI_2 and MZI_{1c}	20–29	P_{31} (1560.0)		54.5
	30–39		P_{31} and P_{32}	54.5 and 54.7
	40–89	P_{32} (1561.8)		54.7
	90–99		P_{32} and P_{33}	54.7 and 54.2
	100–149	P_{33} (1563.6)		54.2
	150–159		P_{33} and P_{34}	54.2 and 55.1
	160	P_{34} (1565.4)		55.1

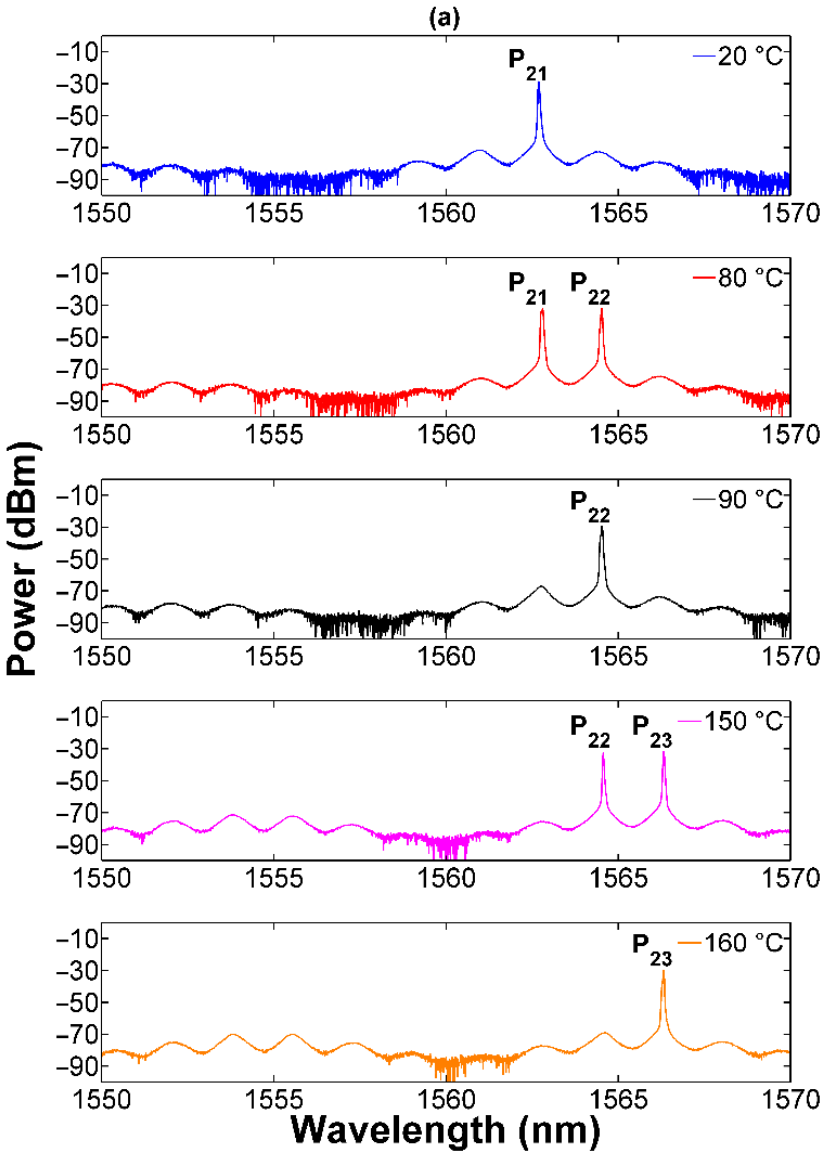

Figure 6. *Cont.*

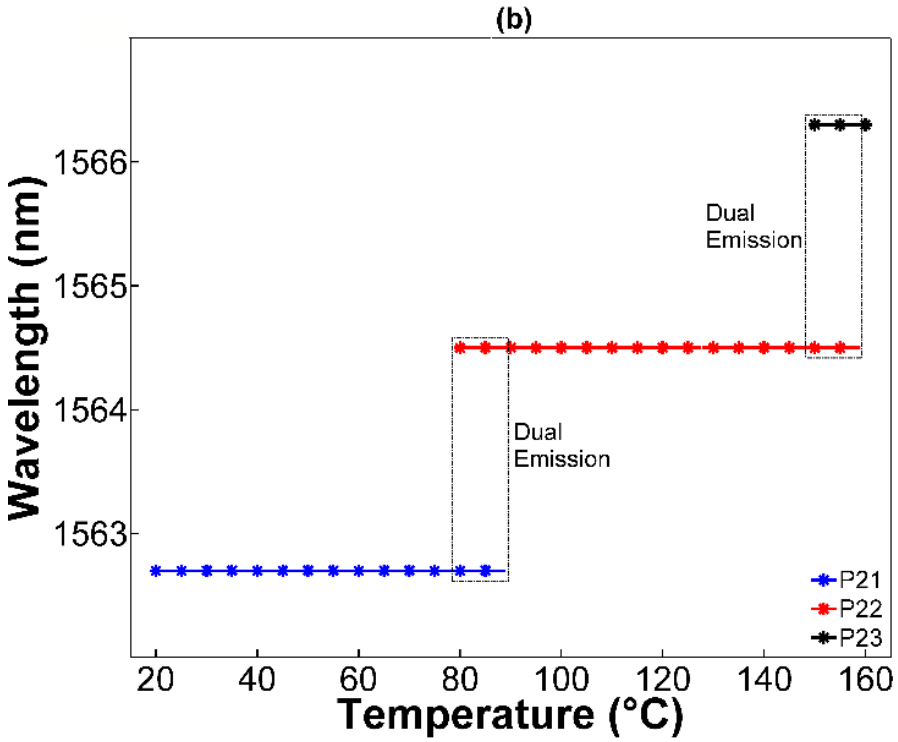

Figure 6. Switchable operation of the EDFL using MZI_2 and MZI_{1b} in a cascade configuration, withstanding temperature variations between 20 to 160 °C. (**a**) Laser emissions and (**b**) stability analysis of laser emissions against temperature changes.

3.3. MZI_2 and MZI_{1c} in a Cascade Configuration

The transmission spectrum of the cascaded MZI_2 and MZI_{1c} is shown in Figure 4c. The peak that shows the highest transmission is likely to produce the laser emission of the EDFL; in this case, P_{31}. In the laser cavity, these two interferometers were connected in a series configuration (see Figure 1). The pump power was fixed at 250 mW and both interferometers were at 20 °C. Laser emission was observed at 1560.0 nm (P_{31}), with an SNR of 54.5 dB, as shown in Figure 7a. An analysis similar to that of the previous cases was performed by increasing the temperature of the MZI_{1c} in increments of 1 °C, from 20 to 160 °C (see Figure 7a,b). The linewidth of P_{31}, P_{32}, P_{33}, and P_{34} was 0.03 nm. The general results of the measurement are shown in Table 3. It is worth noting that as the *FSR* of MZI_1 was reduced, the wavelength switching range increased, as can be observed from Figures 5–7. First, it is necessary to say that the temperature sensitivity of the three MZI_1 is around 33 pm/°C; therefore, the wavelength shift as a function of temperature for these filters is the same. From Figure 2a–c, one may observe that the MZI_{1a}, with the larger *FSR*, also exhibits a larger plateau at its peak, compared with the MZI_{1b} and MZI_{1c}. Since the plateau is larger, we need a more significant wavelength shift to observe laser switching, which translates to a small number of laser switching transitions for a given temperature range. On the other hand, in the case of MZI_{1c}, which has a smaller *FSR* and a sharper peak (smaller plateau), the number of laser switching transitions increases significantly for the same temperature range; therefore, a smaller *FSR* (i.e., sharper spectrum) provides more laser transitions.

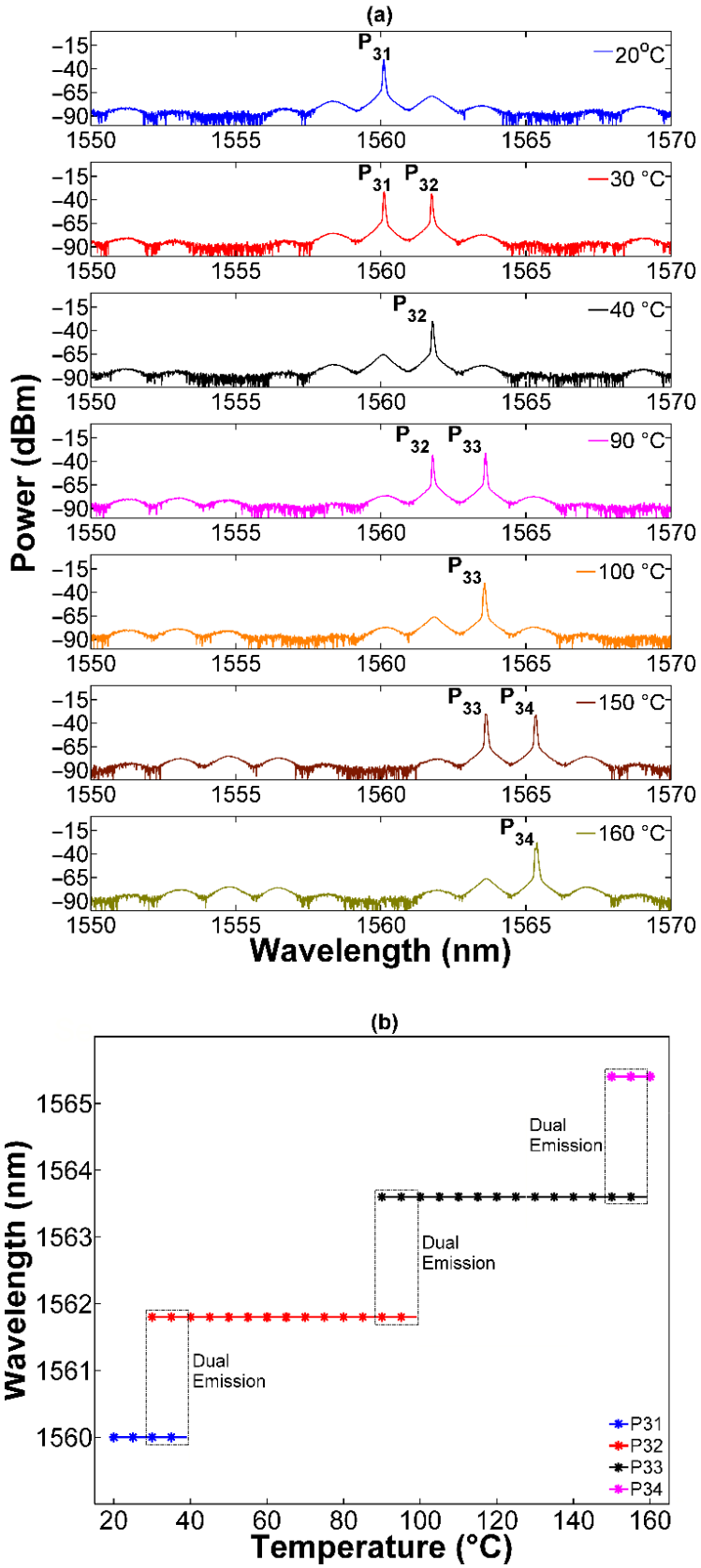

Figure 7. Switchable operation of the EDFL using MZI_2 and MZI_{1c} in a cascaded configuration, withstanding temperature variations between 20 to 160 °C. (**a**) Laser emissions and (**b**)stability analysis of laser emissions against temperature changes.

4. Discussion

The experimental results regarding the switchable operation of the EDFL for the three possible combinations of the MZI_2 with the MZI_{1a}, MZI_{1b}, and MZI_{1c}, respectively, are summarized in Table 3. Regarding single-wavelength laser emissions, they were detected twice in the first combination of MZI_2 and MZI_{1a}, at peaks P_{11} and P_{12}; in the second combination of MZI_2 and MZI_{1b}, they were identified three times, at peaks P_{21}, P_{22}, and P_{23}, and in the third combination of MZI_2 and MZI_{1c}, it was detected four times, at peaks P_{31}, P_{32}, P_{33}, and P_{34}. For the case of dual-wavelength laser emissions, it was detected once in the first combination of MZI_2 and MZI_{1a}, at peaks P_{11} and P_{12}. In the second combination of MZI_2 and MZI_{1b}, it was observed twice, at P_{21} and P_{22}, and P_{22} and P_{23}. In the third combination of MZI_2 and MZI_{1c}, it was identified three times, at P_{31} and P_{32}, P_{32} and P_{33}, and P_{33} and P_{34}. Regarding dual-wavelength switchable operations, they were detected by decreasing the *FSR* of the MZI_1 and noting the number of times that the dual operation increased in the same temperature range. Similar behavior was observed in the single-wavelength switchable operation (see Table 3). The output power of the laser emissions is another interesting feature of this EDFL that needs to be analyzed. The output power of the laser emissions decreased as the laser switched from single to dual operation, and the power increased when the laser switched from dual to single operation. This is because the power is redistributed on the peaks. When MIZ_{1a} was used in the laser, a maximum power change of 2.2 dBm was measured when switching from single to dual laser emissions, and a maximum power change of 2.7 dBm was measured when switching from dual to single laser emissions. In the case of the MZI_{1b}, maximum power changes of 3.2 and 2.7 dBm were measured when switching from single to dual laser emissions, and from dual to single laser emissions, respectively. In the case of the MZI_{1c}, the maximum power changes when switching from single to dual laser emissions and from dual to single laser emissions were the same, at 3.7 dBm.

It should be noted that the most significant characteristic of the proposed EDFL is that it can be switched from lasing single to dual wavelengths by increasing the temperature of the MZI_1. This performance offers an advantage over the switchable laser based on polarization [10–13,23], not only because of its simple straight-line operation but also because of its stability against temperature fluctuations. Switchable lasers based on polarization have a problem with temperature fluctuations, and these fluctuations produce changes in the polarization state; therefore, small adjustments need to be applied to the polarization controller to keep the wavelength and amplitude of the laser emission. However, the laser emissions of this switchable laser exhibited fluctuations in wavelength and power when the temperature of the MZI_1 was changed within a certain temperature range. These experimental results would appear to indicate that a highly accurate temperature controller is not required to regulate the temperature of the MZI_1, since temperature oscillations of up to 9 °C do not change the wavelength or amplitude of the single or dual wavelengths, and in some cases, this temperature value can be even larger (see Table 3). This can be achieved due to the small size of both MZIs. It is worth noting that the level linearity and wavelength linearity of the OSA are 0.05 dB and ±10 pm, respectively; this means that our equipment is not able to detect power or wavelength fluctuations that are lower than the values mentioned above. It is important to highlight two vital features of this proposed switchable EDFL, which both come from the use of the MZI_2. The first one is related to the linewidth of 0.03 nm for all the laser emissions, although the other interferometers (MZI_{1a}, MZI_{1b}, and MZI_{1c}) have different *FSR* values. The second is the fact that the wavelength spacing between dual-wavelength laser emissions is always 1.8 nm, which is the *FSR* of the MZI_2.

Table 4 was expanded upon to compare the performance of our laser with that of similar switchable lasers, using recently published studies. It is worth noting that in most of these works (from 1 to 7), a fiber interferometer was constructed using conventional fiber couplers, thus causing the system to become more complex and bulkier. The laser linewidth of our switchable laser is narrower than 2, 6, and 7, but wider than 3, 4, and 8.

Regarding the SNR, its value is higher than all the lasers in Table 4. These striking results demonstrate the good performance of our switchable laser.

Table 4. Laser parameter comparison using recently published works.

No.	Structure	Switchable Lines	SMSR/NSR	Linewidth
1 [26]	MZI (bi-tapered) and Sagnac (Coupler)	5	NA/>14.98 dB	NA
2 [10]	Sagnac (coupler) and Filter (PMF)	3	NA/23 dB	<600 pm
3 [25]	MZI (coupler) and Filter (TCPCF)	2	>45 dB/NA	26 pm
4 [28]	MZI (coupler) and MZI (TSCF)	1	45 dB/NA	17.1 pm
5 [27]	Filter (SE-HSOFF) and Sagnac (coupler)	4	NA/>30 dB	NA
6 [29]	MZI (Coupler) and Sagnac (Coupler)	5	48.7 dB/NA	60 pm
7 [30]	NOLM (Coupler) and Filter (Lyot)	23	>25 dB/NA	500 pm
8 [13]	Filter (FLCSCF)	6	NA/>50 dB	20 pm
This work	MZI (CHCF) and MZI (CHCF)	2	NA/58.9 dB	30 pm

5. Conclusions

This paper has proposed and experimentally demonstrated the use of a single and dual-wavelength EDFL, incorporating two MZIs, in a series configuration. The all-fiber MZIs were constructed by splicing a section of a capillary hollow core fiber (CHCF) between two segments of MMF. These MZIs exhibit good characteristics, such as ease of construction, small size, low cost, and robustness when being handled. Moreover, their interference patterns have contrast well and do not change with the input polarization's state of light (polarization-independent element). Moreover, an MZI with a longer *FSR*, was used as a wavelength selector, whereas an MZI with a shorter *FSR* made the linewidths narrower and determined the size of the switchable step. The novelty of this single and dual-wavelength EDFL is that the switchable operation of the laser is achieved by thermally tuning the interference pattern of the MZI, and not by adjusting the polarization state inside the fiber ring cavity. The maximum measured value of SNR was 58.9 dB for the single and dual-wavelength laser emissions, and the linewidth of all the peaks was 30 pm. Furthermore, no power or wavelength fluctuations were detected during the single and dual-wavelength operation, making the laser emissions of this switchable EDFL highly stable. The good performance of this switchable EDFL makes it a candidate for potential application in optical fiber communications systems and fiber sensing.

Author Contributions: Conceptualization, I.H.-R., D.A.M.-A. and L.A.H.-P.; methodology, L.A.H.-P., D.A.M.-A. and I.H.-R.; validation, I.H.-R., D.A.M.-A., L.A.H.-P. and S.M.-G.; formal analysis, L.A.H.-P., D.A.M.-A. and I.H.-R.; investigation, L.A.H.-P. and S.M.-G.; resources, I.H.-R., V.P.M. and M.T.-C.; software, S.M.-G.; data curation, L.A.H.-P. and I.H.-R.; writing—original draft preparation, I.H.-R. and L.A.H.-P.; writing—review and editing, S.M.-G., V.P.M., D.A.M.-A. and M.T.-C.; visualization, L.A.H.-P. and S.M.-G.; supervision, I.H.-R.; project administration, I.H.-R.; funding acquisition, I.H.-R., D.A.M.-A. and M.T.-C. All authors have read and agreed to the published version of the manuscript.

Funding: This research was funded by CONACyT, grant numbers CB2017-2018-A1-S-31806, CB2016-286368, and CB2016-286629; in part by UNIVERSIDAD DE GUANAJUATO, grant number CIIC-088/2022.

Data Availability Statement: Not applicable.

Acknowledgments: S. Marrujo-García is grateful to CONACyT for the Ph.D. scholarship. I. Hernández-Romano gratefully acknowledges the generous financial support of Universidad de Guanajuato.

Conflicts of Interest: The authors declare no conflict of interest. The funders had no role in the design of the study; in the collection, analyses, or interpretation of data; in the writing of the manuscript; or in the decision to publish the results.

References

1. Lee, S.-M.; Choi, K.-M.; Mun, S.-G.; Moon, J.-H.; Lee, C.-H. WDM-PON Based on Wavelength-Locked Fabry-Pe/Spl Acute/Rot Laser Diodes. *IEEE Photon. Technol. Lett.* **2005**, *17*, 1579–1581. [CrossRef]
2. Al-Mashhadani, M.K.S.; Al-Mashhadani, T.F.; Goktas, H.H. Broadly Tunable 40 GHz Brillouin Frequency Spacing Multiwavelength Brillouin–Erbium Fiber Laser for DWDM. *Opt. Commun.* **2019**, *451*, 116–123. [CrossRef]
3. Diaz, S.; Lopez-Amo, M. Dual-Wavelength Single-Longitudinal-Mode Erbium Fiber Laser for Temperature Measurements. *Opt. Eng.* **2014**, *53*, 036106. [CrossRef]
4. Li, Y.; Zhou, C.; Tian, J.; Ji, S.; Yao, Y. An All-Fiber Multi-Channel Ultrasonic Sensor Using a Switchable Fiber Bragg Gratings Filter in Erbium-Doped Fiber Laser. *J. Light. Technol.* **2019**, *37*, 4330–4339. [CrossRef]
5. Ahmad, N.A.B.; Dahlan, S.H.; Jamaluddin, M.H.; Sanchez-Lara, R.; Cholan, N.A. A Microwave Signal Generation Technique Based on Brillouin-Erbium Fiber Laser. *Int. J. Integr.* **2019**, *11*, 33–38. [CrossRef]
6. Kumar, A.; Gautam, A.; Priye, V. Microwave Photonic Mixer Using DP-DDMZM for Next Generation 5G Cellular Systems. *Fiber Integr. Opt.* **2020**, *39*, 149–168. [CrossRef]
7. Moon, D.S.; Paek, U.-C.; Chung, Y. Multi-Wavelength Lasing Oscillations in an Erbium-Doped Fiber Laser Using Few-Mode Fiber Bragg Grating. *Opt. Express* **2004**, *12*, 6147. [CrossRef] [PubMed]
8. Liu, Y.; Dong, X.; Shum, P.; Yuan, S.; Kai, G.; Dong, X. Stable Room-Temperature Multi-Wavelength Lasing Realization in Ordinary Erbium-Doped Fiber Loop Lasers. *Opt. Express* **2006**, *14*, 9293. [CrossRef]
9. Chen, W.G.; Lou, S.Q.; Feng, S.C.; Wang, L.W.; Li, H.L.; Guo, T.Y.; Jian, S.S. Switchable Multi-Wavelength Fiber Ring Laser Based on a Compact in-Fiber Mach-Zehnder Interferometer with Photonic Crystal Fiber. *Laser Phys.* **2009**, *19*, 2115–2119. [CrossRef]
10. He, W.; Zhu, L.; Meng, F.; Song, Y.; Dong, M. Selectable and Stable C-Band Multi-Wavelength Ring Cavity Erbium-Doped Fiber Laser Employing Sagnac Loop and Tunable Filter. *Optik* **2019**, *176*, 528–534. [CrossRef]
11. He, W.; Zhu, L.; Dong, M.; Lou, X.; Luo, F. Wavelength-Switchable C-Band Erbium-Doped Fibre Laser Incorporating All-Fibre Fabry–Perot Interferometer Fabricated by Chemical Etching. *J. Mod. Opt.* **2018**, *65*, 818–824. [CrossRef]
12. Martin-Vela, J.A.; Sierra-Hernandez, J.M.; Gallegos-Arellano, E.; Estudillo-Ayala, J.M.; Bianchetti, M.; Jauregui-Vazquez, D.; Reyes-Ayona, J.R.; Silva-Alvarado, E.C.; Rojas-Laguna, R. Switchable and Tunable Multi-Wavelength Fiber Laser Based on a Core-Offset Aluminum Coated Mach-Zehnder Interferometer. *Opt. Laser Technol.* **2020**, *125*, 106039. [CrossRef]
13. Tang, Z.; Liu, L.; Benson, T.; Lian, Z.; Lou, S. Dual-Wavelength Interval Tunable and Multi-Wavelength Switchable High-Performance Fiber Laser Based on Four-Leaf Clover Suspended Core Fiber Filter. *Opt. Laser Technol.* **2021**, *139*, 106966. [CrossRef]
14. Chang, Y.; Pei, L.; Wang, J.; Zheng, J.; Ning, T.; Li, J.; Xie, C. Highly Stable Multi-Wavelength Fiber Laser Based on Hybrid Enclosed Two-Armed Fiber Filter. *Opt. Fiber Technol.* **2022**, *71*, 102894. [CrossRef]
15. Huang, B.; Sheng, X.; Tang, Z.; Lou, S. High SMSR and Widely Tunable Multi-Wavelength Erbium Doped Fiber Laser Based on Cascaded Filters. *Infrared Phys. Technol.* **2022**, *122*, 104082. [CrossRef]
16. Liu, X.; Zhan, L.; Luo, S.; Wang, Y.; Shen, Q. Individually Switchable and Widely Tunable Multiwavelength Erbium-Doped Fiber Laser Based on Cascaded Mismatching Long-Period Fiber Gratings. *J. Light. Technol.* **2011**, *29*, 3319–3326. [CrossRef]
17. Silva-Alvarado, E.C.; Martinez-Rios, A.; Gallegos-Arellano, E.; Martin-Vela, J.A.; Ledesma-Carrillo, L.M.; Reyes-Ayona, J.R.; Porraz-Culebro, T.E.; Sierra-Hernandez, J.M. Tunable Filter Based on Two Concatenated Symmetrical Long Period Fiber Gratings as Mach-Zehnder Interferometer and Its Fiber Lasing Application. *Opt. Laser Technol.* **2022**, *149*, 107824. [CrossRef]
18. Wang, F.; Xu, E.-M.; Dong, J.-J.; Zhang, X.-L. A Tunable and Switchable Single-Longitudinal-Mode Dual-Wavelength Fiber Laser Incorporating a Reconfigurable Dual-Pass Mach–Zehnder Interferometer and Its Application in Microwave Generation. *Opt. Commun.* **2011**, *284*, 2337–2340. [CrossRef]
19. Wei, H.; Lianqing, Z.; Mingli, D. All-Fiber Mach–Zehnder Comb Filter Based on Tapered Fibers for Wavelength Switchable Erbium-Doped Fiber Lasers. *Int. J. Optomechatron.* **2020**, *14*, 18–28. [CrossRef]
20. Zhao, Q.; Pei, L.; Tang, M.; Xie, Y.; Ruan, Z.; Zheng, J.; Ning, T. Switchable Multi-Wavelength Erbium-Doped Fiber Laser Based on Core-Offset Structure and Four-Wave-Mixing Effect. *Opt. Fiber Technol.* **2020**, *54*, 102111. [CrossRef]
21. Zhao, Q.; Pei, L.; Zheng, J.; Tang, M.; Xie, Y.; Li, J.; Ning, T. Switchable, Widely Tunable and Interval-Adjustable Multi-Wavelength Erbium-Doped Fiber Laser Based on Cascaded Filters. *J. Light. Technol.* **2020**, *38*, 2428–2433. [CrossRef]
22. Zou, H.; Lou, S.; Yin, G.; Su, W. Switchable Dual-Wavelength PM-EDF Ring Laser Based on a Novel Filter. *IEEE Photon. Technol. Lett.* **2013**, *25*, 1003–1006. [CrossRef]
23. Lv, Y.; Lou, S.; Tang, Z.; Liu, X.; Wang, X. Tunable C-Band and L-Band Multi-Wavelength Erbium-Doped Fiber Ring Laser Based on a Triple-Core Photonic Crystal Fiber with Polarization-Dependent Loss. *Opt. Laser Technol.* **2020**, *128*, 106269. [CrossRef]
24. Qi, Y.; Kang, Z.; Sun, J.; Ma, L.; Jin, W.; Lian, Y.; Jian, S. Wavelength-Switchable Fiber Laser Based on Few-Mode Fiber Filter with Core-Offset Structure. *Opt. Laser Technol.* **2016**, *81*, 26–32. [CrossRef]
25. Tang, Z.; Lou, S.; Wang, X. Stable and Widely Tunable Single-/Dual-Wavelength Erbium-Doped Fiber Laser by Cascading a Twin-Core Photonic Crystal Fiber Based Filter with Mach-Zehnder Interferometer. *Opt. Laser Technol.* **2019**, *109*, 249–255. [CrossRef]
26. He, W.; Yuan, H.; Lou, X.; Zhu, L.; Dong, M. Multi-Wavelength Switchable Erbium-Doped Fiber Laser Based on a Hybrid Filter Incorporating a Bi-Tapered Mach–Zehnder Interferometer and Sagnac Loop. *Phys. Scr.* **2019**, *94*, 125502. [CrossRef]
27. Chang, Y.; Pei, L.; Ning, T.; Zheng, J.; Li, J.; Xie, C. Switchable and Tunable Multi-Wavelength Fiber Ring Laser Employing a Cascaded Fiber Filter. *Opt. Fiber Technol.* **2020**, *58*, 102240. [CrossRef]

28. Zhang, L.; Tian, Z.; Chen, N.-K.; Han, H.; Liu, C.-N.; Grattan, K.T.V.; Rahman, B.M.A.; Zhou, H.; Liaw, S.-K.; Bai, C. Room-Temperature Power-Stabilized Narrow-Linewidth Tunable Erbium-Doped Fiber Ring Laser Based on Cascaded Mach-Zehnder Interferometers with Different Free Spectral Range for Strain Sensing. *J. Light. Technol.* **2020**, *38*, 1966–1974. [CrossRef]
29. Filoteo-Razo, J.D.; Hernandez-Garcia, J.C.; Estudillo-Ayala, J.M.; Pottiez, O.; Jauregui-Vazquez, D.; Sierra-Hernandez, J.M.; Lauterio-Cruz, J.P.; Carrillo-Delgado, C.M.; Rojas-Laguna, R. Multi-Wavelength Er–Yb-Doped Fibre Ring Laser Using a Double-Pass Mach–Zehnder Interferometer with a Sagnac Interferometer. *Opt. Laser Technol.* **2021**, *139*, 106994. [CrossRef]
30. Xin, L.; Zhou, X.; Chen, J. Low Threshold Multi-Wavelength Erbium-Doped Fiber Ring Laser with NOLM and Lyot Filter. *Opt. Fiber Technol.* **2022**, *68*, 102800. [CrossRef]
31. Marrujo-García, S.; Hernández-Romano, I.; May-Arrioja, D.A.; Minkovich, V.P.; Torres-Cisneros, M. In-Line Mach–Zehnder Interferometers Based on a Capillary Hollow-Core Fiber Using Vernier Effect for a Highly Sensitive Temperature Sensor. *Sensors* **2021**, *21*, 5471. [CrossRef] [PubMed]
32. Marrujo-García, S.; Herrera-Piad, L.A.; Hernández-Romano, I.; May-Arrioja, D.A.; Minkovich, V.P.; Torres-Cisneros, M. Narrow Spectral Linewidth and Tunable Erbium-Doped Fiber Ring Laser Using a MZI Based on CHCF. *Opt. Fiber Technol.* **2021**, *67*, 102739. [CrossRef]